

GSK3 β inhibits epithelial-mesenchymal transition *via* the Wnt/ β -catenin and PI3K/Akt pathways

Cheng Zhang¹, Li Su^{1,2,3}, Li Huang¹, Zheng-Yu Song^{1,4}

¹Department of Ophthalmology, Shanghai General Hospital (Shanghai First People's Hospital), Shanghai Jiao Tong University School of Medicine, Shanghai 200000, China

²Shanghai Key Laboratory of Fundus Diseases, Shanghai 200000, China

³Shanghai Engineering Center for Visual Science and Photomedicine, Shanghai 200000, China

⁴Department of Ophthalmology, Shanghai Shuguang Hospital, Shanghai University of Traditional Chinese Medicine, Shanghai 200000, China

Co-first authors: Cheng Zhang and Li Su

Correspondence to: Zheng-Yu Song. Department of Ophthalmology, Shanghai Shuguang Hospital, Shanghai University of Traditional Chinese Medicine, Shanghai 200000, China. rockersong@126.com

Received: 2018-03-02 Accepted: 2018-05-08

Abstract

• **AIM:** To investigate the regulatory mechanism of glycogen synthase kinase 3 β (GSK3 β) in epithelial-mesenchymal transition (EMT) process after proliferative vitreoretinopathy (PVR) induction.

• **METHODS:** Experimental PVR was induced by intravitreal injection of retinal pigment epithelium (RPE) cells in the eyes of rabbits. A PI3K/Akt inhibitor (wortmannin) and a GSK3 β inhibitor (LiCl) were also injected at different time during PVR progress. Electroretinogram (ERG), ocular fundus photographs, and B-scan ultrasonography were used to observe the PVR progress. Western blot test on the extracted retina were performed at 1, 2, 4wk. The expression of the mesenchymal marker vimentin was determined by immunohistochemistry. Toxicity of wortmannin and LiCl were evaluated by ERG and TdT-mediated dUTP nick-end labeling (TUNEL) assay. The vitreous was also collected for metabolomic analysis.

• **RESULTS:** Experimental PVR could significantly lead to EMT, along with the suppressed expression of GSK3 β and the activation of Wnt/ β -catenin and PI3K/Akt pathways. It was verified that upregulating the expression of GSK3 β could effectively inhibit EMT process by suppressing Wnt/ β -catenin and PI3K/Akt pathways.

• **CONCLUSION:** GSK3 β effectively inhibits EMT *via* the Wnt/ β -catenin and PI3K/Akt pathways. GSK3 β may

be regarded as a promising target of experimental PVR inhibition.

• **KEYWORDS:** epithelial-mesenchymal transition; experimental proliferative vitreoretinopathy; glycogen synthase kinase 3 β ; rabbits

DOI:10.18240/ijo.2018.07.08

Citation: Zhang C, Su L, Huang L, Song ZY. GSK3 β inhibits epithelial-mesenchymal transition *via* the Wnt/ β -catenin and PI3K/Akt pathways. *Int J Ophthalmol* 2018;11(7):1120-1128

INTRODUCTION

Proliferative vitreoretinopathy (PVR) is the most common cause of failed retinal detachment (RD) surgery, with an incidence of 5%-10%^[1]. During the PVR process, the formation of fibrotic membranes within the subretinal, retinal surface, and intravitreal space could lead to failed retinal reattachment^[2]. The pathogenesis of fibrotic membranes is characterized by excessive proliferation and retinal migration of cells, such as retinal pigment epithelium (RPE) cells, macrophages and glial cells^[3]. The primary cellular change in fibrotic membranes is transdifferentiation from RPE cells to myofibroblasts through epithelial-mesenchymal transition (EMT)^[4]. Many *in vitro* experiments have focused on individual cytokines, and demonstrated their inhibitory effects on EMT. However, the individual effect of these cytokines *in vivo* experiment were rarely reported. This indicates that PVR is a complicated process involving multiple cytokines and pathways, and that simply inhibiting one factor or pathway may cause compensatory responses in the body.

The multifunctional serine/threonine kinase glycogen synthase kinase 3 β (GSK3 β) is involved in multiple signaling pathways and pathophysiological processes, such as EMT, differentiation, motility, inflammation, proliferation, and metabolism^[5-6]. GSK3 β participates in the suppression of a variety of diseases, including cancer, Alzheimer's disease, and diabetes^[7-8]. The functional activity of GSK3 β will be activated due to the inhibition of PI3K [wortmannin (WOR)]^[9]. Nevertheless, the mechanism of GSK3 β action in EMT has not been fully elucidated.

In addition, most previous studies of the pathological mechanism of EMT induced by PVR have focused solely on protein levels, without *in vivo* analysis of metabolites, which are the end products of biological fluids, cells, or tissues.

Their levels represent a comprehensive response to biological systems or environmental changes, and can be used as potential biomarkers in a number of pathological diseases^[10]. Therefore, we have investigated the role of GSK3 β in EMT with metabolomic analysis *in vivo* experiment.

SUBJECTS AND METHODS

Animals and Proliferative Vitreoretinopathy Induction

Adult New Zealand white rabbits (72 in total; 2.0-2.5 kg) were obtained from the Shanghai Laboratory Animal Center at the Chinese Academy of Sciences, and maintained in a 12h light/dark cycle. Food and water were supplied *ad libitum*. All animal experiments in this study conformed to the Association for Research in Vision and Ophthalmology Statement for the Use of Animals in Ophthalmic and Vision Research. Briefly, after 1wk of accommodation, PVR was induced by intravitreal injection of 1.0×10^6 human ARPE19 cells in 0.1 mL buffered salt solution (BSS) with a 30-gauge needle (after anterior chamber paracentesis) as previously described^[11].

Drug Injection and Observation We randomly selected 42 rabbits, whose right eyes were injected with 0.3 mmol/L WOR (Selleckchem 52758; Houston, TX, USA), a phosphoinositol-3 kinase (PI3K) inhibitor. They were further randomly separated into equal groups with three different injection times: 3d before PVR induction, during induction, and 7d afterwards (the PW3B, PW, and PW7A groups, respectively). The left eyes of all 42 rabbits were injected with WOR without PVR induction. Another 14 rabbits were randomly selected and injected with 5 mmol/L LiCl (Sigma L9650; St Louis, MO, USA), a pharmacological GSK3 β inhibitor, in their right eyes at the same time as PVR induction (the PL group). Their left eyes were injected with LiCl without PVR induction. The remaining 16 rabbits were injected intravitreally with BSS (0.1 mL) in their right eyes, and their left eyes are used as uninjected controls. Note that all rabbits maintained normal intraocular pressure after intravitreal treatment. Clinical observations with an indirect ophthalmoscope were performed 1, 7, 14, 21, and 28d after PVR induction. At the same time points, vitreous and retinal samples were extracted for study.

Western Blot Analysis To detect GSK3 β , phosphorylated (p)-GSK3 β , β -catenin, α -smooth muscle actin (α -SMA), vimentin, E-cadherin, samples were homogenized in 100 μ L of ice-cold radio-immunoprecipitation assay (RIPA) buffer supplemented with the proteinase inhibitor phenylmethanesulfonyl fluoride (PMSF 100 mmol/L). Retina homogenates (40 μ g of protein) were then separated by sodium dodecyl sulfate-polyacrylamide gel electrophoresis and transferred to polyvinylidene difluoride membranes. After blocking nonspecific sites with 5% bovine serum albumin, the membranes were probed with the following primary antibodies: α -SMA (ab7817, Abcam, Cambridge, MA, USA), vimentin (sc-6260, Santa Cruz, Dallas, TX, USA), E-cadherin (ab6528, Abcam, Cambridge, MA, USA), Akt

(cst 9271, New England Biolabs), p-Akt Ser473 (cst 9271, New England Biolabs), GSK3 β (sc-7291, Santa Cruz, Dallas, TX, USA), p-GSK3 β Ser9 (sc-373800, Santa Cruz, Dallas, TX, USA), and β -catenin (sc-7963, Santa Cruz, Dallas, TX, USA) and detected with anti-mouse or anti-rabbit secondary antibodies conjugated to horseradish peroxidase (HRP; Jackson Immuno Research Laboratories) for 1h each. Bands were visualized using Amersham Imager 600 system (GE Healthcare Bio-Sciences AB, Uppsala, Sweden). Analyses of the relative protein levels were evaluated by Image J software (NIH).

Nuclear Magnetic Resonance Spectroscopy For metabolomics analysis by nuclear magnetic resonance (NMR), the vitreous fluid was collected and stored immediately at -80°C . The samples were dissolved in 600 μ L of phosphate buffer (0.2 mol/L $\text{Na}_2\text{HPO}_4/0.2$ mol/L NaH_2PO_4 , pH 7.4), and then centrifuged at $11\,000 \times g$ for 10min at 4°C . Aliquots of the supernatant (500 μ L) were transferred to 5 mm NMR tubes, and 50 μ L of D_2O was added for NMR measurements. ^1D proton spectra were recorded using the water-suppressed Carr-Purcell-Meiboom-Gill (CPMG) pulse sequence [RD- 90° -(τ - 180° - τ)n-ACQ]. A fixed total spin-spin relaxation delay 2 nr of 120ms was used to attenuate the broad NMR signals of slowly tumbling molecules with short T_2 relaxation times and to retain signals of low-molecular weight compounds. All ^1H NMR spectra were acquired by a Bruker AVANCE III NMR spectrometer, operated at 600.18 MHz for 1h. Spectra were obtained using the pulse sequence (RD-90-t1-90-tm-90-ACQ). Measurements for all samples were performed at 25°C .

Clinical Observation Examinations using indirect ophthalmoscopy, ocular fundus imaging, and B-scan ultrasonography were performed 28d after PVR induction. PVR was graded from 0 to 5, according to the Fastenberg classification^[12].

Histology and Immunohistochemistry Rabbits were sacrificed and their eyeballs were enucleated and fixed in 4% formaldehyde +1.5% glutaraldehyde for at least 73h. The eyeballs were then embedded in paraffin. A segment including the PVR scars was selected, and cross-sectioned to 5 μ m thickness. The retina sections were stained with hematoxylin and eosin (H&E). For immunohistochemical analysis, sections were incubated with mouse anti-vimentin antibodies (sc-6260, Santa Cruz, Dallas, TX, USA) at 4°C overnight. After washing the slides three times, sections were labeled with HRP-conjugated sheep anti-mouse IgG for 50min, followed by staining with 3,3'-diaminobenzidine (Beyotime; brown).

Safety Evaluation The potential retinal toxicity of WOR and LiCl was evaluated by TUNEL assay and electroretinogram (ERG). Moreover, possible toxicity was examined daily by indirect ophthalmoscopy. Animals receiving intravitreal WOR or LiCl were examined by ERG 28 d after injection, and then enucleated for TUNEL analysis.

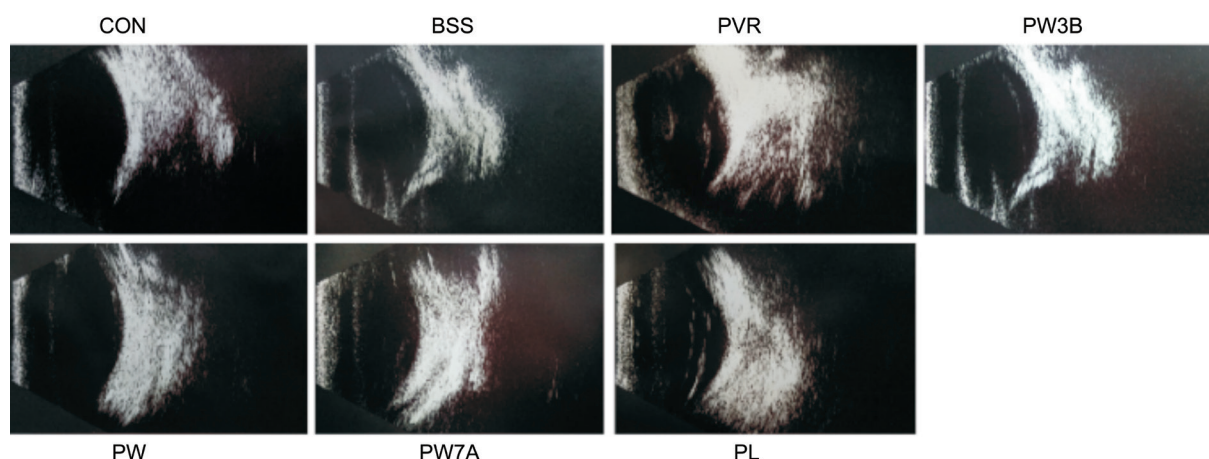


Figure 1 B-scan examination at 28d after PVR induction.

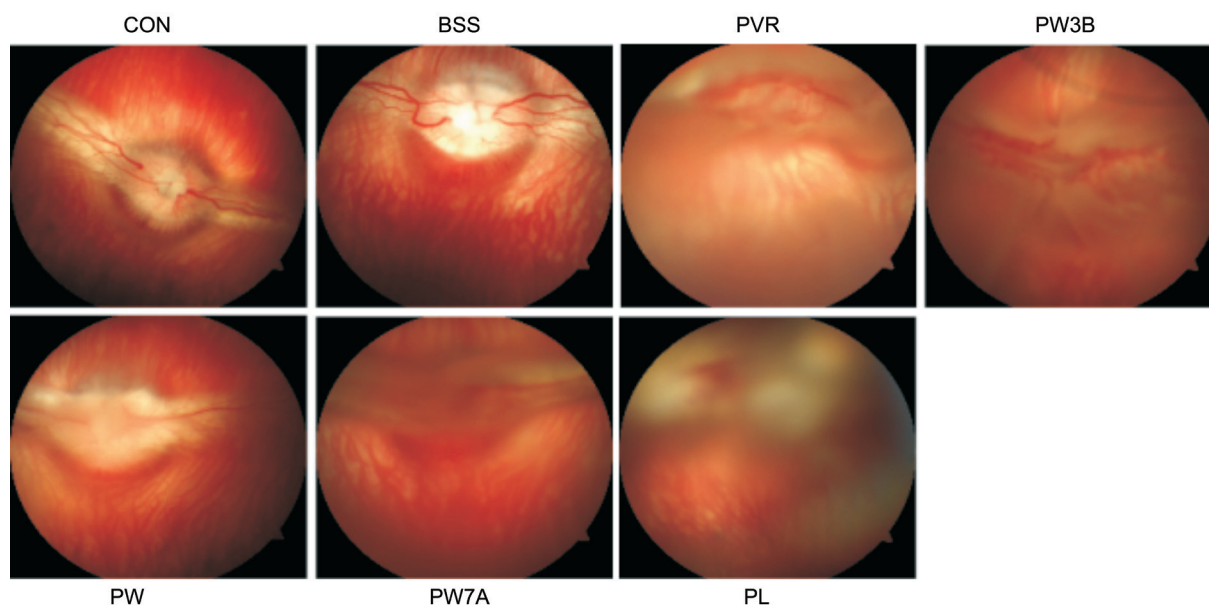


Figure 2 Effects of GSK-3 β on the clinical manifestation at 28d after PVR induction.

TdT-mediated dUTP Nick-end Labeling Assay To examine the toxicity of WOR and LiCl, paraffin-embedded retinal tissue sections were deparaffinized, rehydrated, fixed with 4% paraformaldehyde for 15min at 4°C, and subjected to enzymatic digestion with proteinase K for 25min at room temperature. Induction of apoptosis was detected using the TUNEL Assay Kit (Roche 11684817910), according to the manufacturer's instructions.

Electroretinogram To evaluate the severity of PVR and toxicity of WOR and LiCl, ERG were performed 1d before the injection and 7 and 28d after. The pupils of the rabbits' eyes were dilated with 5% tropicamide. The rabbits were then placed in a dark room for 30min for dark adaption. Rabbits were then anesthetized, and corneal contact lens electrodes were placed on the corneal surfaces over a layer of 1% methylcellulose gel. All these procedures were performed in dim red light. Standard white flash stimulation of the retina was performed in a scotopic background and the scotopic 0 dB ERGs were recorded. To minimize variability, the ratios of the scotopic b-wave amplitudes of the treated eyes compared to control or pre-injected eyes were used as indices of retinal function.

Statistical Analysis All results are expressed as means \pm standard errors of the mean (SEM). The statistical significance among multiple groups was determined by analysis of variance; $P < 0.05$ was considered statistically significant. All experiments were performed at least three times.

RESULTS

B-scan Examination and Fundus Imaging We also acquired B-scans 28d after PVR induction, and noted folding of the detached retina in the PVR and PL groups. However, in the WOR-treated groups, obvious funicular echo was not observed. Similar to fundus imaging, this demonstrated that the PI3K inhibitor could relieve the severity of PVR (Figure 1). And we also performed indirect ophthalmoscopic examinations and acquired fundus images 28d after the injection to look for evidence of traction and RD. We observed detachment of both medullary wings with significant vitreous traction in the PVR group. Additionally, the PL group displayed severe vessel distortion and blurry optic nerves. By contrast, proliferation was significantly inhibited in the WOR-treated groups (Figure 2).

Electroretinogram Evaluation ERGs were obtained the day before the injection and 1, 7, and 28d after injection to evaluate retinal function. To minimize variability, the ratios of the B-wave amplitudes of the WOR-injected and LiCl-injected eyes to those of pre-injection eyes were used as indices of retinal function. As shown in Figure 3, compared with the control and BSS groups, the B-wave ratios of the PW3B, PW, PW7A, and PL groups all decreased after 1, 7, and 28d. In the PL group, the B-wave ratio decreased significantly to 0.35, on day 28 compared to the control group, while the PVR group ratio was 1.11. The ratios of the PW3B, PW, and PW7A groups were all between the control and PVR groups.

Down-regulation of the GSK3 β and Activation of the Signaling Pathways after PVR Induction Total Akt levels were stable in all groups 7, 14, and 28d after injection of RPE cells. However, compared to the control and BSS-injection groups, the PVR induction group revealed significant time-dependent increases in β -catenin, p-Akt (Ser473), and p-GSK3 β (Ser9). Meanwhile, there was a decrease in total GSK3 β demonstrated in the PVR group (Figure 4). These results suggest that the GSK3 β were down-regulated during PVR induction. Moreover, PI3K/Akt and Wnt/ β -catenin signaling pathways are involved in PVR process.

Epithelial-mesenchymal Transition after Experimental Proliferative Vitreoretinopathy Induction After intravitreal injection of RPE cells, EMT was measured based on changes in protein expression. Retinas were screened by Western blot analysis to examine the expression of the epithelial marker E-cadherin, and the mesenchymal markers α -SMA and vimentin. E-cadherin was downregulated 7, 14, and 28d after PVR induction, while α -SMA and vimentin were significantly upregulated (Figure 5).

Effects of Wortmannin and LiCl on the GSK3 β Expression and Signaling Pathways To further examine the mechanism underlying the effects of WOR, p-Akt, p-GSK3 β , GSK3 β , and β -catenin were examined by Western blot (Figure 6). As expected, WOR treatment increased the expression of total GSK3 β and abrogated the observed increases in β -catenin, p-Akt (Ser473), and p-GSK3 β (Ser9) in the PVR group. LiCl treatment caused the opposite effect compared with WOR treatment. As a conclusion, the WOR treatment effectively caused activation of GSK3 β and inhibited the activity of the PI3K/Akt and Wnt/ β -catenin pathways.

Suppression of EMT in Experimental Proliferative Vitreoretinopathy by Injection of Wortmannin To further evaluate the role of GSK3 β in PVR, intravitreal injection with either WOR or LiCl was performed alongside RPE cell injection. Then, α -SMA, vimentin, and E-cadherin protein levels were assessed by Western blot. As shown in (Figure 7) in the WOR-treated group, the expression of α -SMA and vimentin was markedly decreased and the expression of E-cadherin was

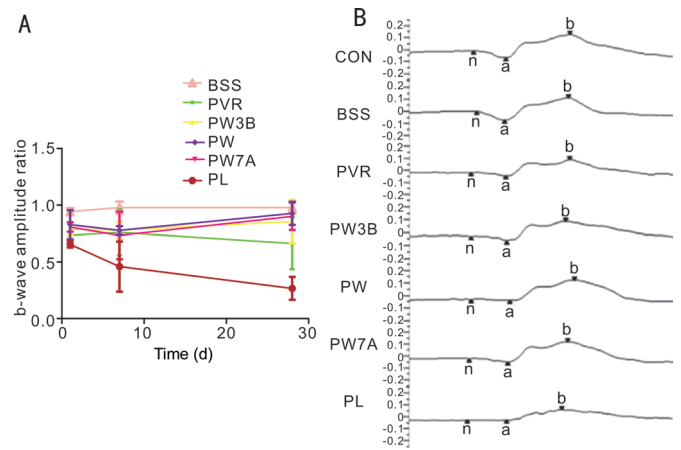


Figure 3 ERG evaluation A: ERG evaluation between groups. The ratios of the b-wave amplitudes of the WOR or LiCl injected eyes to those of the normal control of pre-injection eyes were used as indices of retinal function; B: Representative scotopic ERGs from each group on day 28.

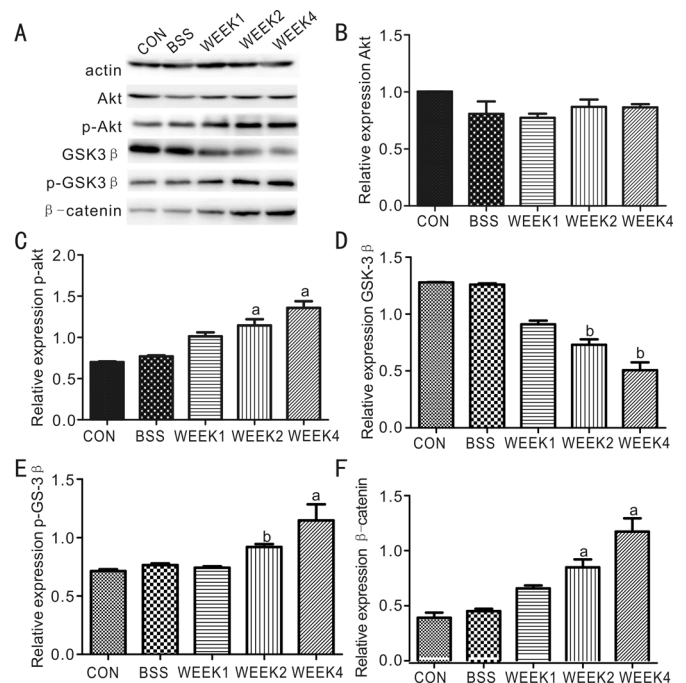


Figure 4 Down-regulation of the GSK3 β and activation of the signaling pathways after PVR induction Western blot showed the protein levels of Akt, p-Akt, GSK3 β , p-GSK3 β , β -catenin. EMT expression after PVR induction. ^aStatistical significance ($P<0.05$) compared with control group; ^bStatistical significance ($P<0.01$) compared with control group.

increased compared with the PVR and PL groups. Conversely, EMT was enhanced by inhibition of GSK3 β .

Immunohistochemical Analysis By immunohistochemistry, the PVR group expressed significantly more vimentin than the control group at 28d (Figure 8). Consistent with the Western blot results, the analysis revealed that the WOR-treated groups (PW3B, PW, and PW7A) expressed less vimentin than the PVR and PL groups.

Wortmannin and LiCl Toxicity The toxicity of intravitreal injection of WOR and LiCl was examined by TUNEL assay

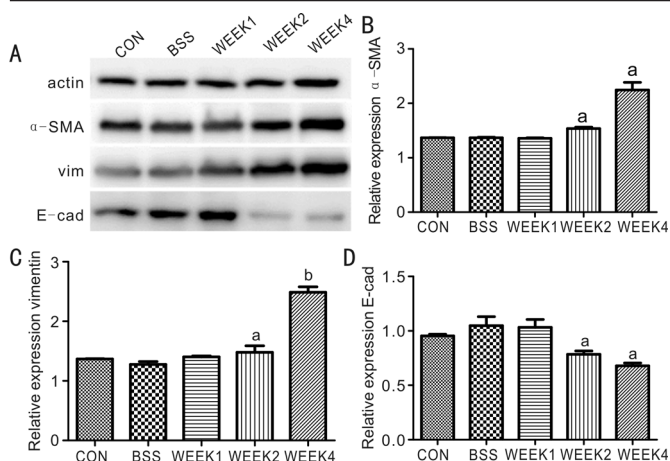


Figure 5 The expression levels of α -SMA, vimentin, and E-cadherin were detected by Western blot ^aStatistical significance ($P < 0.05$) compared with control group; ^bStatistical significance ($P < 0.01$) compared with control group.

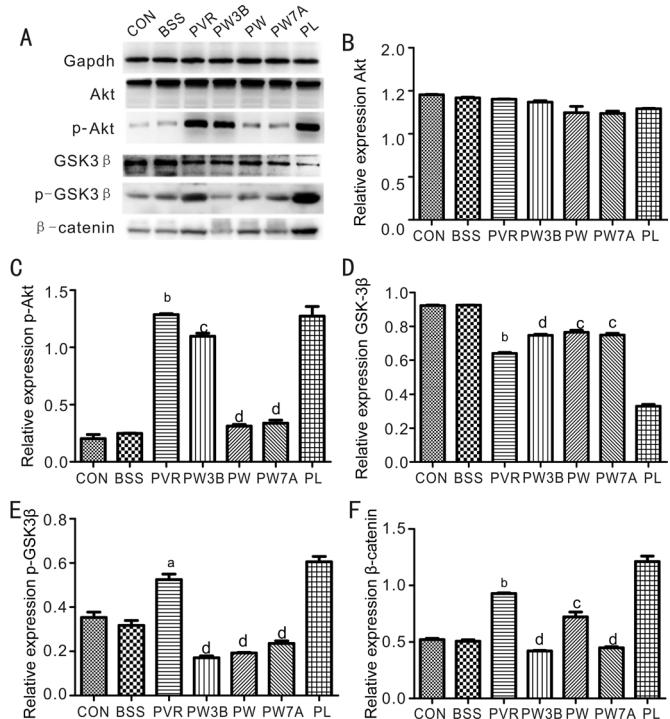


Figure 6 Western blot analysis of GSK3 β expression and signaling pathways after WOR or LiCl intervention Western blot showed protein levels of Akt, p-Akt, GSK3 β , p-GSK3 β , β -catenin. ^aStatistical significance ($P < 0.05$) compared with control group; ^bStatistical significance ($P < 0.01$) compared with control group; ^cStatistical significance ($P < 0.05$) compared with PVR group; ^dStatistical significance ($P < 0.01$) compared with PVR group.

(Figure 9A) and ERG (Figure 9B) during the 28d observation period. The TUNEL assay showed no evidence of apoptosis, and in ERG examination, WOR and LiCl did not affect the amplitudes of each waveform. No evidence of toxicity was found in the rabbit retina.

Multivariate Analysis of ¹H NMR Spectra of Vitreous Metabolites The ¹H-NMR spectra of vitreous samples were recorded to exploit quantitative metabolic information and then subjected to multivariate data analysis. An unsupervised

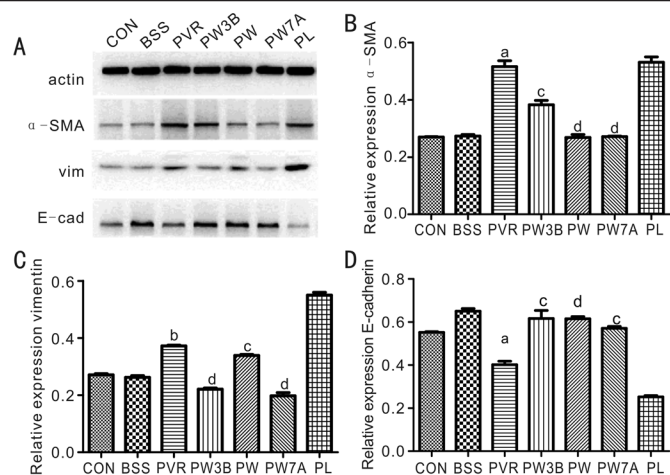


Figure 7 Western blot analysis of EMT effects in PVR after WOR or LiCl intervention Western blot showed protein levels of α -SMA, vimentin, and E-cadherin. ^aStatistical significance ($P < 0.05$) compared with control group; ^bStatistical significance ($P < 0.01$) compared with control group; ^cStatistical significance ($P < 0.05$) compared with PVR group; ^dStatistical significance ($P < 0.01$) compared with PVR group.

pattern recognition method, principal component analysis (PCA) (Figure 10A, 10E, 10I, 10M, and 10Q), was first performed to explore the metabolic profiles differences among groups. Then the supervised clustering analysis of partial least squares discriminant analysis (PLS-DA) (Figure 10B, 10F, 10J, 10N and 10R) was conducted to enhance the separations in the PCA. The parameters of Q2 (cum) and R2X (cum) were computed to test the validity of the models, and the results indicated that the PLS-DA model was reliable and suitable for metabolomics analysis. Moreover, orthogonal partial least squares discriminant analysis (OPLS-DA) was employed to modify the PLS-DA method. Those metabolites with the absolute value of r greater than 0.576, VIP value bigger than 1, and/or the P values obtained from Wilcoxon test exceeding 0.05 were used to identify variables that were responsible for the discrimination of groups. This analysis indicated a clear separation between each group in the determination of metabolic differences (Figure 10C, 10G, 10K, 10O and 10S). Heat plots between the groups are presented in Figure 10D, 10H, 10L, 10P, and 10T, and these dendrograms show the presence of different subclusters with different numbers of metabolites. Lastly, in order to explore the metabolic profile differences among the groups, a PCA plot with all groups (Figure 11A) and batch analysis plot (Figure 11B) were generated.

Biomarker Identification The average changes of metabolites between groups were calculated by using the normalized integral, *i.e.* $(C_A - C_B)/C_B$, where C_A and C_B embody the mean metabolite integrals of two groups. A list of discriminative metabolites is provided in Table 1, which showed an increase in glycine, valine, lysine, and branched-chain amino acids in

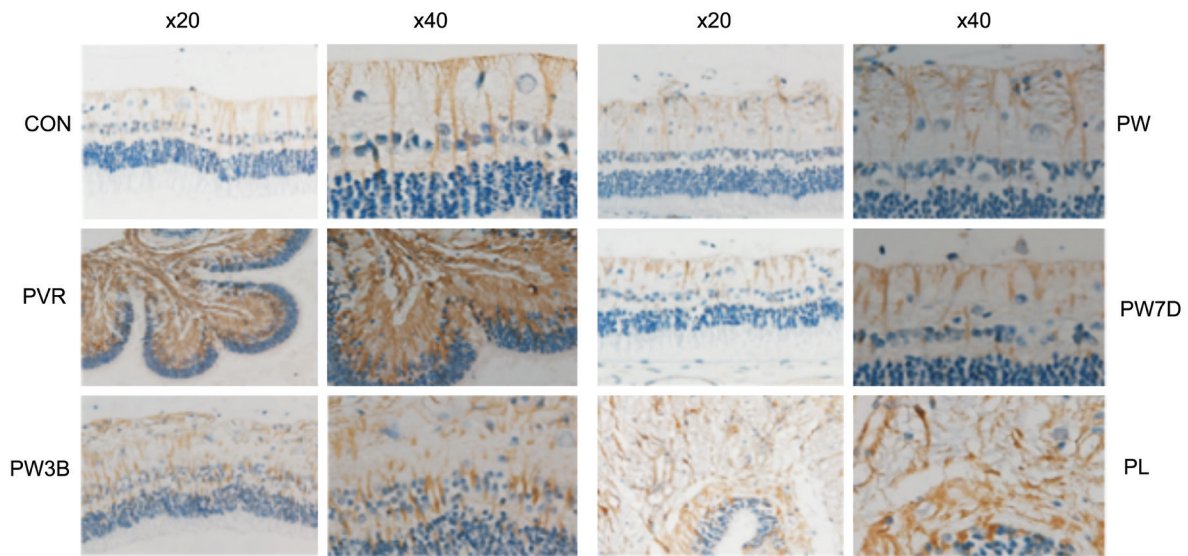


Figure 8 Immunohistochemical analysis showed effects of GSK-3 β on the expression of vimentin after PVR induction 20 \times , 40 \times enlarged. Safety evaluation of WOR or LiCl.

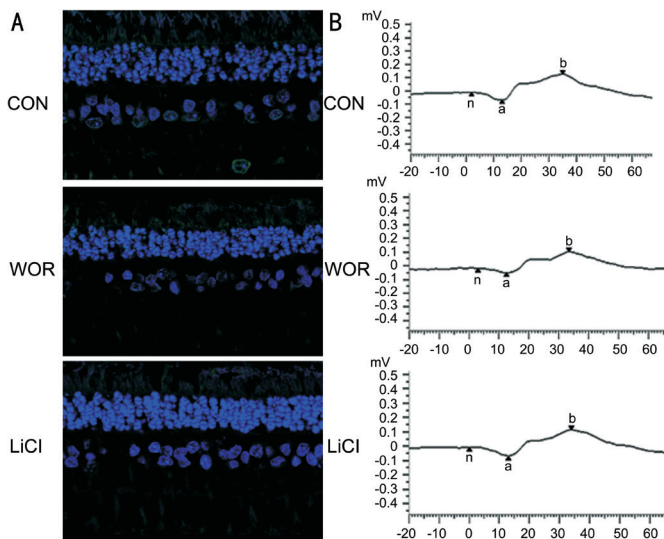


Figure 9 Representative immunofluorescence images of TUNEL-positive (green) retinal cells at 28d after WOR or LiCl injection A: Scale bar, 50 μ m; B: Individual typical ERG recordings of the three groups at 28d.

PVR group compared with the control group. Meanwhile the WOR treatment decrease these amino acids compared with PVR group.

DISCUSSION

Our results suggest that the severity of EMT can be attenuated by upregulating the expression of GSK3 β , which blocks the Wnt/ β -catenin and PI3K/Akt pathways, and indicate that GSK3 β could be a potential clinical target in the treatment of PVR.

We found that GSK3 β expression was significantly reduced during the development of experimental PVR. To further clarify the function of GSK3 β during PVR progression, GSK3 β was activated and inhibited, respectively, by intravitreal injection of WOR or LiCl. Moreover, WOR was injected at three different times: 3d before induction, during induction,

and 7d afterwards (in the PW3B, PW, and PW7A groups). The results showed that upregulating the expression of GSK3 β in three different times all have inhibitory EMT effects, indicating the potential value of targeting GSK3 β in clinical applications. Furthermore, we conducted metabolomic analysis to verify our conclusion. Metabolomics can analyze all metabolite changes from complete biological systems rather than individual cells, allowing assessment of a variety of metabolic pathways^[13]. Our ¹H-NMR analyses revealed increases in glycine, valine, lysine, and branched-chain amino acids (BCAAs; Table 1), contrary to previous studies^[14]. This is mostly due to the ubiquitin-proteasome pathway (UPP)-mediated degradation of abundant vitreous proteins. Experimental PVR progresses with increased proliferation, inflammation, oxidation, and nutrient consumption^[15-16]. With biochemical adaptation, the degradation of multiple vitreous proteins is aggravated, providing adequate amino acids for gluconeogenesis, new protein synthesis, and energy production. The increased turnover and degradation of proteins is also observed in uremia and patients with cancer cachexia^[17-18]. Our results demonstrate that compared with the PVR and PL groups, the metabolite profiles of the WOR-treated groups were closer to the control group. While the PL group presented more serious degradation of proteins in comparison with the PVR group. The metabolomics analysis demonstrates that GSK3 β regulation can significantly affect EMT development, and that after GSK3 β stimulation, the metabolite changes are similar to the control group.

To clarify how GSK3 β plays its role in inhibiting EMT during PVR, we assessed the activation of Wnt/ β -catenin and PI3K/Akt pathways. As the critical and canonical Wnt pathway, the Wnt/ β -catenin pathway participates in cell proliferation, differentiation, and various biological processes^[19-20]. GSK3 β is the most important kinase and negative regulatory factor

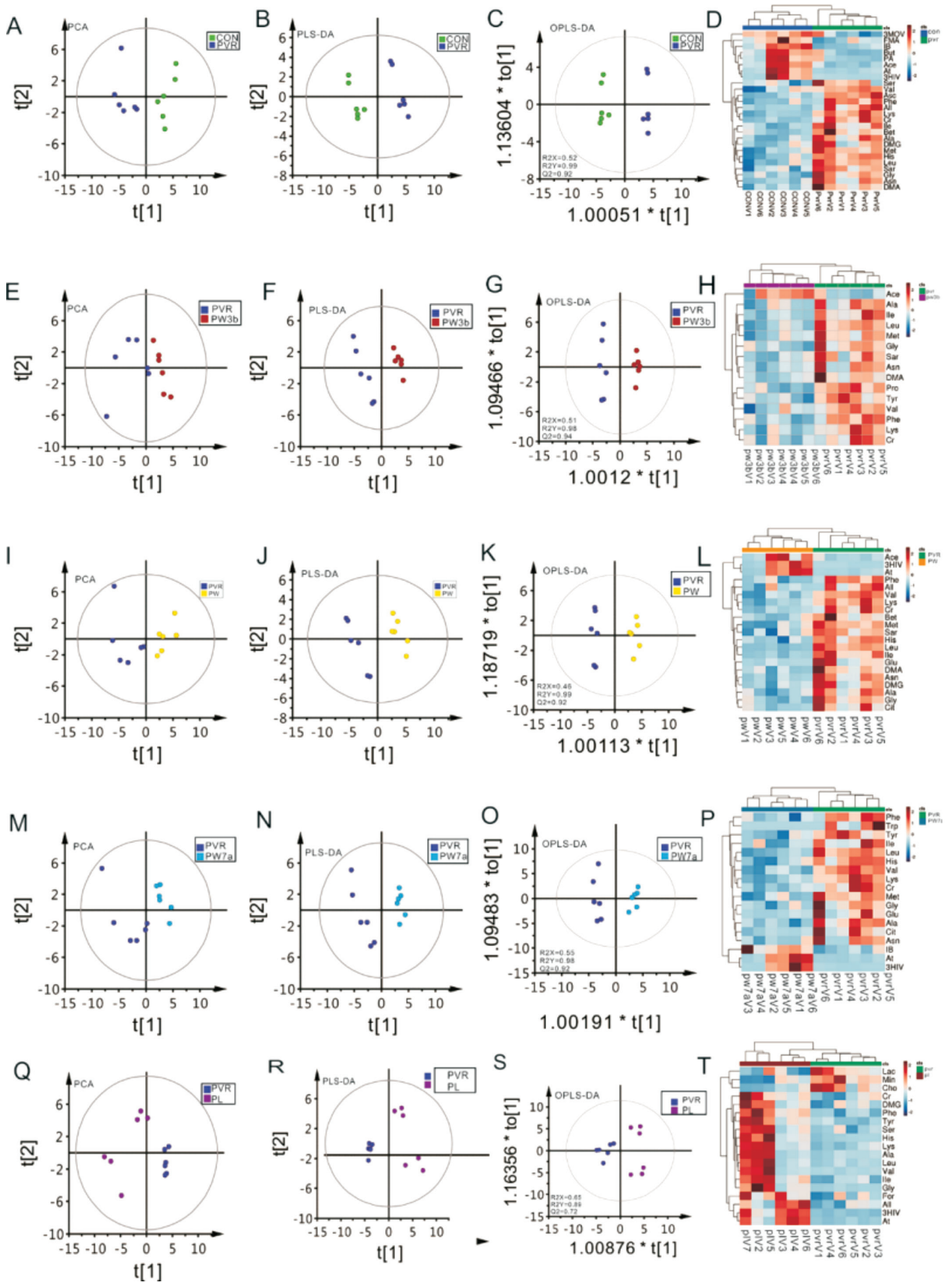


Figure 10 The score plots of PCA, PLS-DA, and OPLS-DA analysis of NMR spectra A-D: CON vs PVR group; E-H: PVR vs PW3B group; I-L: PVR vs PW group; M-P: PVR vs PW7A group; Q-T: PVR vs PL group.

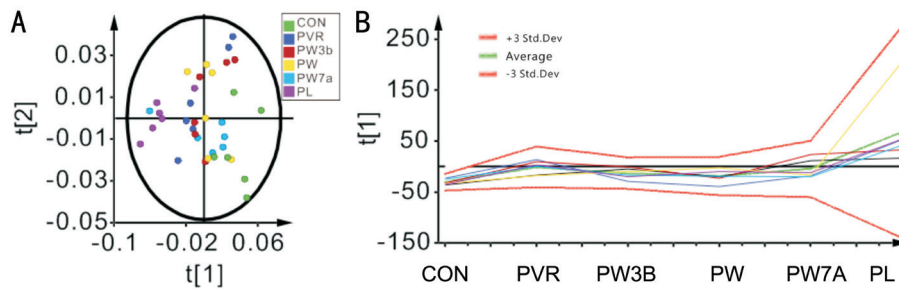


Figure 11 The PCA plot (A) and batch analysis plot (B) among groups.

Table 1 The average changes of metabolites between groups

Metabolites	Fold (^a t , VIP, ^b P)				
	PVR vs CON	PW3B vs PVR	PW vs PVR	PW7A vs PVR	PL vs PVR
All	+2.65 (0.75, 1.18, 0)	<i>P</i> >0.05	-0.55 (0.62, 0.96, 0.04)	<i>P</i> >0.05	+1.03 (0.68, 1.18, 0.03)
Ala	+0.49 (0.83, 1.32, 0)	-0.24 (0.67, 1.3, 0.02)	-0.31 (0.78, 1.32, 0)	-0.39 (0.87, 1.42, 0)	+1.17 (0.6, 1.14, 0.04)
Asn	+1.66 (0.73, 1.18, 0.01)	-0.49 (0.64, 1.32, 0.02)	<i>P</i> >0.05	-0.45 (0.65, 1.21, 0.04)	<i>P</i> >0.05
Bet	+1.02 (0.74, 1.19, 0.01)	<i>P</i> >0.05	-0.39 (0.65, 1.13, 0.03)	<i>P</i> >0.05	<i>P</i> >0.05
Cr	+1.22 (0.84, 1.29, 0)	-0.33 (0.66, 1.16, 0.03)	-0.44 (0.81, 1.26, 0)	-0.41 (0.8, 1.27, 0)	+0.54 (0.77, 1.22, 0.02)
DMA	+1.89 (0.69, 1.08, 0.01)	-0.52 (0.61, 1.23, 0.03)	-0.67 (0.67, 1.14, 0.01)	<i>P</i> >0.05	<i>P</i> >0.05
DMG	+1.16 (0.63, 1.12, 0.04)	<i>P</i> >0.05	-0.64 (0.67, 1.21, 0.01)	<i>P</i> >0.05	+0.9 (0.68, 1.18, 0.04)
Gly	+0.66 (0.79, 1.23, 0)	-0.33 (0.75, 1.43, 0.01)	-0.39 (0.79, 1.32, 0)	-0.28 (0.7, 1.22, 0.01)	+3.86 (0.67, 1.16, 0.02)
His	+1.35 (0.91, 1.39, 0)	<i>P</i> >0.05	-0.4 (0.88, 1.41, 0)	-0.35 (0.86, 1.4, 0)	+1.96 (0.68, 1.17, 0.01)
Ile	+0.87 (0.75, 1.25, 0)	-0.49 (0.76, 1.42, 0)	-0.62 (0.85, 1.36, 0)	-0.35 (0.64, 1.08, 0.03)	+1.01 (0.75, 1.25, 0.01)
Leu	+0.76 (0.87, 1.34, 0)	-0.35 (0.84, 1.51, 0)	-0.52 (0.95, 1.49, 0)	-0.43 (0.91, 1.49, 0)	+0.96 (0.6, 1.13, 0.03)
Lys	+1.12 (0.91, 1.39, 0)	-0.3 (0.76, 1.34, 0.01)	-0.48 (0.9, 1.4, 0)	-0.41 (0.88, 1.4, 0)	+0.69 (0.69, 1.2, 0.02)
Met	+0.9 (0.81, 1.24, 0)	-0.31 (0.66, 1.24, 0.01)	-0.6 (0.82, 1.29, 0)	-0.5 (0.78, 1.32, 0)	<i>P</i> >0.05
Phe	+0.74 (0.79, 1.2, 0)	-0.49 (0.81, 1.41, 0)	-0.46 (0.79, 1.25, 0)	-0.44 (0.79, 1.29, 0.01)	+1.11 (0.81, 1.29, 0)
Val	+0.47 (0.75, 1.14, 0.01)	-0.22 (0.68, 1.19, 0.01)	-0.37 (0.91, 1.43, 0)	-0.35 (0.89, 1.43, 0)	+1.97 (0.57, 1.09, 0.04)

PVR: Proliferative vitreoretinopathy; PW3B: 3d before PVR induction group; PW: During induction group; PW7A: 7d afterwards group; PL: PVR induction group. ^aThe absolute values of the coefficient number extracted from the S-plot of OPLS-DA models; ^bThe *P* value were obtained from a nonparametric test of Wilcoxon test.

in the Wnt signaling pathway^[21]. Inhibition of GSK3 β leads to the accumulation of β -catenin, which activates the Wnt/ β -catenin pathway^[22-23]. The PI3K/Akt pathway is associated with cell transformation, migration, adhesion, transcription, proliferation, metabolism, and the development of human cancer^[24-25]. Notably, we found that β -catenin and p-Akt were increased during PVR development, while activation of GSK3 β markedly prevented the accumulation of β -catenin and p-Akt and attenuated EMT. This demonstrates that GSK3 β could alleviate the severity of EMT by regulating the Wnt/ β -catenin and PI3K/Akt pathways. Based on this, we propose that traumatic PVR leads to the activation of RPE cells, macrophages and glial cells, which downregulate GSK3 β , activating the Wnt/ β -catenin and PI3K/Akt signaling pathways, and leading to further fibroblast proliferation, metabolomic changes, collagen synthesis, and EMT development. Certainly, how macrophages and glial cells downregulate GSK3 β remains to be investigated in a future study.

There are a few limitations to this study. Firstly, the fundamental differences between rabbits and humans must be acknowledged. Secondly, to better understand the underlying

mechanism causing PVR, the establishment of WOR treatment time points should be more precise and the sample size for all the groups should be increased. Lastly, our metabolomic analysis was limited to the 28d time point, without analysis of acute and long-term chronic metabolomic changes, which also warrant further study. However, our study has demonstrated that GSK3 β inhibits EMT in experimental PVR by regulating the Wnt/ β -catenin and PI3K/Akt pathways. These results support our hypothesis and provide new evidence supporting the clinical targeting of these signaling pathways.

In conclusion, our study has demonstrated that GSK3 β could inhibit EMT in experimental PVR by regulating the Wnt/ β -catenin and PI3K/Akt pathways. Thus, these results may provide a new promising therapeutic strategy for PVR disease.

ACKNOWLEDGEMENTS

Foundations: Supported by the National Natural Science Foundation of China (No.81371039); Shanghai Natural Science Foundation (No.18ZR1440200).

Conflicts of Interest: Zhang C, None; Su L, None; Huang L, None; Song ZY, None.

REFERENCES

- 1 Pastor JC, Rojas J, Pastor-Idoate S, Di Lauro S, Gonzalez-Buendia L, Delgado-Tirado S. Proliferative vitreoretinopathy: a new concept of disease pathogenesis and practical consequences. *Prog Retin Eye Res* 2016;51:125-155.
- 2 Kwon OW, Song JH, Roh MI. Retinal detachment and proliferative vitreoretinopathy. *Dev Ophthalmol* 2016;55:154-162.
- 3 Tosi GM, Marigliani D, Romeo N, Toti P. Disease pathways in proliferative vitreoretinopathy: an ongoing challenge. *J Cell Physiol* 2014;229(11):1577-1583.
- 4 Tamiya S, Kaplan HJ. Role of epithelial-mesenchymal transition in proliferative vitreoretinopathy. *Exp Eye Res* 2016;142:26-31.
- 5 Li CY, Wang Q, Shen S, Wei XL, Li GX. Oridonin inhibits migration, invasion, adhesion and TGF- β 1-induced epithelial-mesenchymal transition of melanoma cells by inhibiting the activity of PI3K/Akt/GSK-3 β signaling pathway. *Oncol Lett* 2018;15(1):1362-1372.
- 6 Karmali R, Chukkapalli V, Gordon LI, Borgia JA, Ugolkov A, Mazar AP, Giles FJ. GSK-3 β inhibitor, 9-ING-41, reduces cell viability and halts proliferation of B-cell lymphoma cell lines as a single agent and in combination with novel agents. *Oncotarget* 2017;8(70):114924-114934.
- 7 Zhang Y, Huang NQ, Yan F, Jin H, Zhou SY, Shi JS, Jin F. Diabetes mellitus and Alzheimer's disease: GSK-3 β as a potential link. *Behav Brain Res* 2018;339:57-65.
- 8 Saraswati AP, Ali Hussaini SM, Krishna NH, Babu BN, Kamal A. Glycogen synthase kinase-3 and its inhibitors: potential target for various therapeutic conditions. *Eur J Med Chem* 2018;144:843-858.
- 9 Tang D, Chen QB, Xin XL, Aisa HA. Anti-diabetic effect of three new norditerpenoid alkaloids in vitro and potential mechanism via PI3K/Akt signaling pathway. *Biomedicine & pharmacotherapie* 2017;87:145-152.
- 10 Newgard CB. Metabolomics and metabolic diseases: where do we stand? *Cell Metab* 2017;25(1):43-56.
- 11 Wong CA, Potter MJ, Cui JZ, Chang TS, Ma P, Maberley AL, Ross WH, White VA, Samad A, Jia W, Hornan D, Matsubara JA. Induction of proliferative vitreoretinopathy by a unique line of human retinal pigment epithelial cells. *Can J Ophthalmol* 2002;37(4):211-220.
- 12 Fastenberg DM, Diddie KR, Sorgente N, Ryan SJ. A comparison of different cellular inocula in an experimental model of massive periretinal proliferation. *Am J Ophthalmol* 1982;93(5):559-564.
- 13 Rattray NJW, Deziel NC, Wallach JD, Khan SA, Vasiliou V, Ioannidis JPA, Johnson CH. Beyond genomics: understanding exposotypes through metabolomics. *Hum Genomics* 2018;12(1):4.
- 14 Huang L, Zhang C, Su L, Song Z. GSK3 β attenuates TGF- β 1 induced epithelial-mesenchymal transition and metabolic alterations in ARPE-19 cells. *Biochem Biophys Res Commun* 2017;486(3):744-751.
- 15 Jin Y, Chen H, Xu X, Hu Y, Wang C, Ma Z. Traumatic proliferative vitreoretinopathy: clinical and histopathological observations. *Retina* 2017;37(7):1236-1245.
- 16 Tikhonovich MV, Erdiakov AK, Gavrilova SA. Nonsteroid anti-inflammatory therapy suppresses the development of proliferative vitreoretinopathy more effectively than a steroid one. *Int Ophthalmol* 2017.
- 17 Norton JA, Stein TP, Brennan MF. Whole body protein synthesis and turnover in normal man and malnourished patients with and without known cancer. *Ann Surg* 1981;194(2):123-128.
- 18 Jeevanandam M, Horowitz GD, Lowry SF, Brennan MF. Cancer cachexia and protein metabolism. *Lancet* 1984;1(8392):1423-1426.
- 19 Hu Y, Yu K, Wang G, Zhang D, Shi C, Ding Y, Hong D, Zhang D, He H, Sun L, Zheng JN, Sun S, Qian F. Lanatoside C inhibits cell proliferation and induces apoptosis through attenuating Wnt/ β -catenin/c-Myc signaling pathway in human gastric cancer cell. *Biochem Pharmacol* 2018;150: 280-292.
- 20 Wang L, Zhao Y, Wu Q, Guan Y, Wu X. Therapeutic effects of β -elemene via attenuation of the Wnt/ β -catenin signaling pathway in cervical cancer cells. *Mol Med Rep* 2018;17(3):4299-4306.
- 21 Ikeda S, Kishida S, Yamamoto H, Murai H, Koyama S, Kikuchi A. Axin, a negative regulator of the Wnt signaling pathway, forms a complex with GSK-3 β and β -catenin and promotes GSK-3 β -dependent phosphorylation of β -catenin. *EMBO J* 1998;17(5):1371-1384.
- 22 Chen G, Wang D, Zhao X, Cao J, Zhao Y, Wang F, Bai J, Luo D, Li L. miR-155-5p modulates malignant behaviors of hepatocellular carcinoma by directly targeting CTHRC1 and indirectly regulating GSK-3 β -involved Wnt/ β -catenin signaling. *Cancer Cell Int* 2017;17:118.
- 23 Mao Y, Wang L, Zhu Y, Liu Y, Dai H, Zhou J, Geng D, Wang L, Ji Y. Tension force-induced bone formation in orthodontic tooth movement via modulation of the GSK-3 β / β -catenin signaling pathway. *J Mol Histol* 2018;49(1):75-84.
- 24 Liu J, Xing Y, Rong L. miR-181 regulates cisplatin-resistant non-small cell lung cancer via downregulation of autophagy through the PTEN/PI3K/AKT pathway. *Oncol Rep* 2018;39(4):1631-1639.
- 25 Huang Y, Wu S, Zhang Y, Wang L, Guo Y. Antitumor effect of triptolide in T-cell lymphoblastic lymphoma by inhibiting cell viability, invasion, and epithelial-mesenchymal transition via regulating the PI3K/AKT/mTOR pathway. *Oncol Targets Ther* 2018;11:769-779.